β-Site Covalent Reactions Trigger Transitions between Open and Closed Conformations of the Tryptophan Synthase Bienzyme Complex†

Peng Pan and Michael F. Dunn*

Department of Biochemistry, University of California at Riverside, Riverside, California 92521-0129

Received January 4, 1996⊗

ABSTRACT: The tryptophan synthase bienzyme complex ($\alpha_2\beta_2$) from *Salmonella typhimurium* catalyzes the final two steps in the biosynthesis of L-Trp. To investigate the roles played by conformational change in tryptophan synthase catalysis, the fluorophore 8-anilino-1-naphthalenesulfonate (ANS) is used to identify conformational states. The binding of ANS to the $\alpha_2\beta_2$ bienzyme complex is accompanied by a dramatic enhancement of ANS fluorescence and a shift of the emission maximum from 520 to 482 nm. The ANS binding isotherm is biphasic and consists of a class of moderately high-affinity, noninteracting sites with a stoichiometry of 1 site/$\alpha\beta$ dimeric unit ($K_d' = 62 \pm 15$ μM) and a much weaker set of non-specific interactions with $K_d' > 1$ mM. Our findings show that the affinity of the enzyme for ANS is strongly decreased (>10-fold) by interactions at two loci 30 Å apart: (i) the binding of the α-site ligands, 3-indole-D-glycerol 3′-phosphate or α-glycerol phosphate (GP) or (ii) reaction at the β-subunit to form either the α-aminoacrylate Schiff base, E(A-A), or quinonoid species, E(Q). In contrast, formation of the L-Ser and L-Trp external aldimines E(Aex_1) and E(Aex_2) at the β-site causes a 2−3-fold decrease in the affinity of the enzyme for ANS. The combination of E(A-A) or E(Q) with GP brings about almost complete displacement of ANS, indicating that these interactions drive a conformation change in $\alpha\beta$ subunit pairs which prevents the binding of ANS. These results are consistent with a model which postulates that $\alpha\beta$ subunit pairs undergo ligand-mediated transitions between open and closed conformations during the catalytic cycle. Consistent with the kinetic data showing that binding of α-site ligands increases the affinity of the β site for L-Ser and that formation of E(A-A) activates the α reaction [Brzović, P. S., Ngo, K., & Dunn, M. F. (1992) *Biochemistry 31*, 3831−3839], while mutations in α subunit loops 2 and 6 prevent the ligand-mediated transition to a closed structure [Brzović, P. S., Hyde, C. C., Miles, E. W., & Dunn, M. F. (1993) *Biochemistry 32*, 10404−10413], we conclude that reciprocal ligand-mediated allosteric interactions between the heterologous subunits promote conformational transitions between open and closed structures in $\alpha\beta$ subunit pairs which function to coordinate catalytic activities and facilitate the channeling of indole between the two catalytic sites.

The tryptophan synthase from *Salmonella tryphimurium* is a bienzyme complex ($\alpha_2\beta_2$)[1] which catalyzes the final two reactions in the biosynthesis of L-tryptophan (L-Trp) from 3-indole-D-glycerol 3′-phosphate (IGP) and L-serine (L-Ser) (Yanofsky & Crawford, 1972; Miles, 1979; Miles et al., 1987). The α subunit of the bienzyme complex catalyzes the reversible aldolytic cleavage of IGP to D-glyceraldehyde 3′-phosphate (G3P) and indole (α reaction, eq 1). The β subunit catalyzes the pyridoxal 5′-phosphate (PLP) dependent conversion of indole and L-Ser to L-Trp by a β-replacement (β reaction, eq 2). The physiologically important reaction catalyzed by the $\alpha_2\beta_2$ complex ($\alpha\beta$ reaction, eq 3) is the combination of the α and β reactions.

3-indole-D-glycerol 3′-phosphate ⇌ indole + D-glyceraldehyde 3′-phosphate (1)

indole + L-serine ⇌ L-tryptophan + H_2O (2)

3-indole-D-glycerol 3′-phosphate + L-serine ⇌ L-tryptophan + D-glyceraldehyde 3′-phosphate + H_2O (3)

Studies of the catalytic mechanism of the bienzyme complex have been facilitated by use of substrate analogues and site-directed mutagenesis in combination with rapid kinetics. The α active-site residues Glu49 and Asp60 have been reported to play a catalytic role in the α reaction (Yanofsky, 1967; Yanofsky & Crawford, 1972; Yutani et al., 1987; Nagata et al., 1989). The mechanism of the β reaction has been extensively investigated using a variety of spectroscopic, kinetic, and mutational approaches (Miles, 1991a). The chemical steps of the α and β reactions are outlined in Scheme 1.[2]

X-ray crystallography studies have revealed that the α and β active sites are linked by a 25−30-Å long tunnel (Scheme 2) (Hyde et al., 1988). Kinetic studies have demonstrated that the transfer of indole, a product of IGP cleavage at the α site, to the β active site occurs via this tunnel (Dunn et al., 1990; Lane & Kirschner, 1991; Anderson et al., 1991).

† This work was supported by National Science Foundation Grant MCB-9218901.

* To whom correspondence should be addressed.

⊗ Abstract published in *Advance ACS Abstracts,* April 1, 1996.

[1] Abbreviations: ANS, 8-anilino-1-naphthalenesulfonate; IGP, 3-indole-D-glycerol 3′-phosphate; G3P, D-glyceraldehyde 3′-phosphate; GP, α-glycerol phosphate; O-Me-Ser, *O*-methyl-D,L-serine; β-ME, β-mercaptoethanol; $\alpha_2\beta_2$, wild-type tryptophan synthase from *Salmonella typhimurium*; PLP, pyridoxal 5′-phosphate; E(A-A), enzyme-bound Schiff base of α-aminoacrylate; E(Q_1), E(Q_2), and E(Q_3), the L-Ser and L-Trp quinonoidal intermediates (Scheme I); E(Ain), the internal aldimine; E(Aex_1), E(O-MeAex_1), and E(Aex_2), the L-Ser, O-Me-D,L-Ser, and L-Trp external aldimines, respectively; E(GD), geminal diamine intermediate; K_d', apparent dissociation constant.

0006-2960/96/0435-5002$12.00/0

Communication between the α and *β* sites undoubtedly involves ligand-mediated protein conformational changes. The occurrence of ligand-driven conformational transitions of the bienzyme complex implies that both the α and *β* subunits undergo conformational changes during catalysis (Kirschner et al., 1975; Lane & Kirschner, 1983a,b, 1991; Kawasaki et al., 1987; Dunn et al., 1987a,b, 1990; Houben & Dunn, 1990; Anderson et al., 1991; Kirschner et al., 1991; Brzović et al., 1991, 1992a,b, 1993; Leja et al., 1995; Woehl & Dunn, 1995; Ruvinov et al., 1995; Banik et al., 1995). In the α*β* reaction, this conformational transition includes two loop structures that close down over the α site and prevents the escape of indole (Brzović et al., 1992a, 1993). However, details of the relationship between protein structure, ligand binding, conformational change, and catalysis are not well-known.

For a number of proteins, the fluorescent dye 8-anilino-1-naphthalenesulfonate (ANS) has been used successfully as a probe in the investigation of hydrophobic regions and conformational changes. In some instances, ANS was used to probe specific binding sites on the protein (Stryer, 1965; Daniel & Weber, 1966; Brand, 1970). An alternative use of the dye is to investigate ligand−protein interactions that alter the fluorescence of the protein−ANS complex (Bloxham, 1973; Cheung, 1969; Ploug et al., 1994). In this study we report that ANS binds to a hydrophobic region in the bienzyme complex and that the fluorescence of ANS provides a sensitive probe of ligand-driven conformational transitions between protein states.

MATERIALS AND METHODS

Materials. Gly, L-His, L-Ser, L-Trp, *O*-methyl-DL-serine (O-Me-Ser), aniline, ANS, α-glycerol phosphate (GP), and indole were purchased from Sigma. Indoline and triethanolamine were purchased from Aldrich. Indoline was purified by vacuum distillation. *β*-Mercaptoethanol (*β*-ME) was from Calbiochem. Purification of wild-type *Salmonella typhimurium* $\alpha_2\beta_2$ tryptophan synthase and determination of protein concentration have been previously described (Kawasaki et al., 1987; Miles et al., 1987; Miles et al., 1989). IGP was synthesized via an enzyme-catalyzed process and purified as previously described (Kawasaki et al., 1987).

UV-Visible Absorbance and Fluorescence Measurements. The steady-state UV−visible spectral measurements and equilibrium experiments were performed on Hewlett-Packard 8450A and 8452 diode array spectrophotometers. The binding of L-Ser or L-Trp to the *β* site was followed by the changes in absorbance at 350 and 476 nm, respectively. The 350-nm spectral band corresponds to the formation of the

Scheme 1: Mechanisms of the Reactions Catalyzed by the Tryptophan Synthase $\alpha_2\beta_2$ Bienzyme Complex[a]

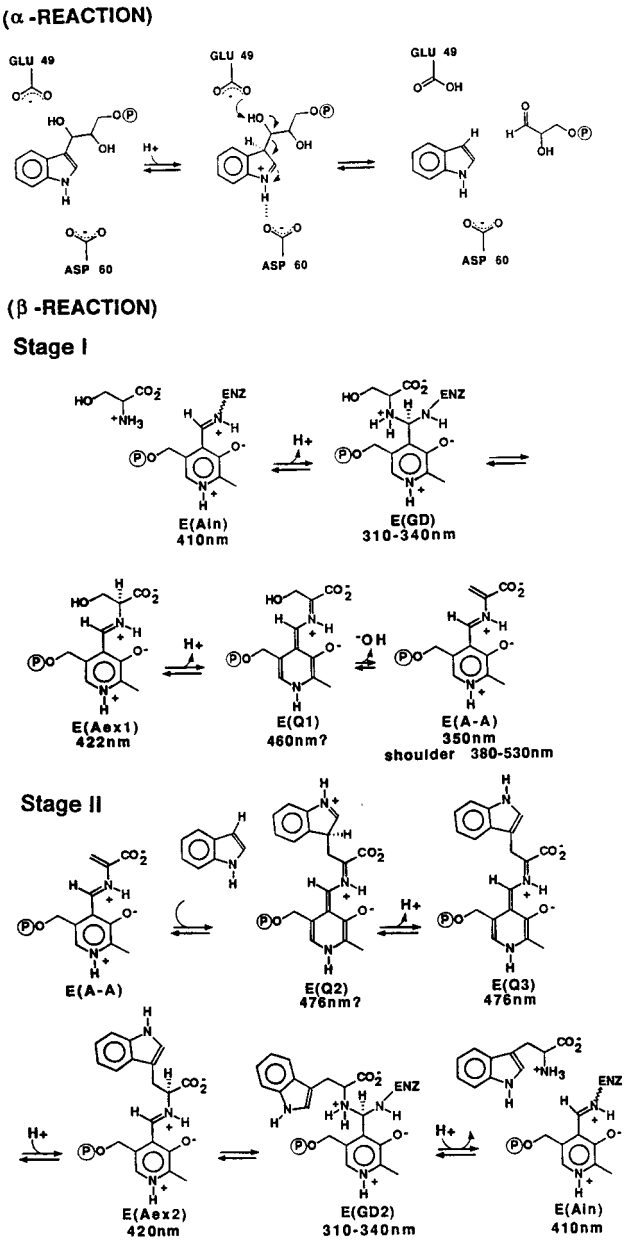

[a] The α reaction shows the cleavage of IGP. The *β* reaction shows the covalent intermediates for the conversion of indole and L-Ser to L-Trp. Absorption maxima for those species which have been characterized are given. The *β*-reaction occurs in two stages, stage I, conversion of L-Ser to the quasi-stable E(A-A), and stage II, conversion of indole and E(A-A) to L-Trp and regeneration of E(Ain)[1]. Reprinted with permission from Leja et al. (1995).

α-aminoacrylate Schiff base, E(A-A), and the 476-nm absorption band is due to the accumulation of the L-Trp quinonoid, $E(Q_3)$ (Drewe & Dunn, 1985, 1986). In some experiments, the binding of ANS was followed by monitoring the difference spectrum changes resulting from the red-shifted absorbance spectrum of enzyme-bound ANS. Difference spectra were calculated by subtracting both the contributions of free ANS and of the enzyme species under study. All experiments were carried out either in 50 mM triethanolamine (TEA) buffer containing 100 mM NaCl (Woehl & Dunn, 1995), pH 7.8, or in 50 mM triethanolamine containing 100 mM NaCl, pH 7.0, at 25 °C. A Spex Fluorolog II spectrofluorometer, equipped with a 150-W Xe source, was used to record fluorescence intensities. Fluorescence emis-

[2] During the *β* reaction, at least eight covalent intermediates with different chemical structures are formed (Scheme 1). The obligatory changes in the structures accompanying interconversion of certain covalent intermediates are coupled to conformational transitions in the *β* site (Drewer & Dunn, 1986; Roy et al., 1988a,b; Houben & Dunn, 1990; Brzović et al., 1992b; Dunn et al., 1994; Leja et al., 1995; Woehl & Dunn, 1995). Efficient catalysis in the $\alpha_2\beta_2$ bienzyme complex necessitates the stabilization of multiple transition states and the destabilization of multiple intermediates along the reaction pathway (Scheme 1) (Pauling, 1948; Drewe & Dunn, 1985; 1986; Roy et al., 1988a,b; Houben et al., 1989). We speculate that all the intermediates along the pathway equilibrate between open and closed subunit conformations and that this interconversion is essential to the biological function of the $\alpha_2\beta_2$ system. Although not proven, it is likely that catalysis at the two sites occurs within the closed subunit conformations, while ligand binding and dissociation occurs via the open conformations.

Scheme 2: Cartoon Depicting the Active Sites of the α and β Subunits, the Interconnecting Tunnel, and the Routes for Entry and Exit of Substrates and Products for the αβ Reaction[a]

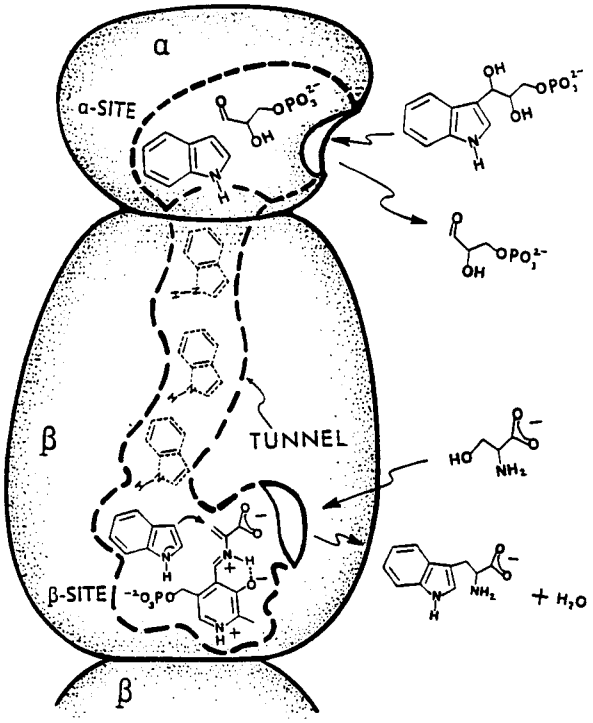

[a] The products of the α reaction (indole and G3P) are shown bound to the α site. The pathway for diffusion of the common metabolite, indole, along the tunnel from the α site to the β site is shown by the three dashed structures. Upon arrival at the β site, indole makes a nucleophilic attack on the α-aminoacrylate Schiff base intermediate. Reprinted with permission from Leja et al. (1995).

sion spectra of ANS were obtained using an excitation wavelength of either 380 or 340 nm, wavelengths where there is little or no change in absorbance during reaction with the substrates and substrate analogues used in this study. Emission spectra were recorded over the range 400−640 nm. To minimize inner cell effects, all fluorescent measurements used a 3 + 3 mm light-path quartz cuvette (Hellma). When the experiments required that measurements be made under conditions where the inner cell effects become significant, empirically determined calibration curves were used to correct the observed fluorescence signals. When the response of the fluorescence of ANS was measured in the reaction of E(A-A) with β-ME as a function of time, fluorescence emission was recorded at a fixed wavelength of 482 nm with an excitation wavelength of 340 nm.

Stopped-Flow Fluorescence and Rapid-Scanning Stopped-Flow (RSSF) Measurements. The fluorescence time courses of rapid binding and displacement of ANS were monitored with an Applied Photophysics microvolume SF.17MV rapid-mixing stopped-flow instrument with customized optical and data acquisition systems. The fluorescence signal was measured as the light emitted through two cutoff filters selected to provide a transmission window from 450 to 550 nm. The excitation wavelength was set at 380 nm. The fluorescence time courses were fit by nonlinear least-squares regression analysis to the sum of exponentials according to the following equation (Bernasconi, 1976):

$$F_t = F_\infty \pm \sum_{i=1}^{n} F_i \exp(-t/\tau_i)$$

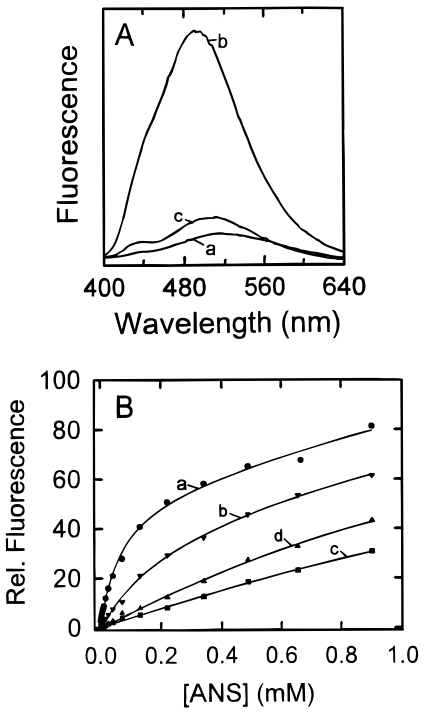

FIGURE 1: Fluorescence emission spectra of free and bound ANS and titration isotherms for ANS binding to tryptophan synthase meausred at pH 7.8 and 25 °C. (A) The emission spectra of samples containing 50 μM ANS were recorded by using an excitation wavelength of 380 nm in the absence of the enzyme (a) and in the presence of 12 μM $\alpha_2\beta_2$ (b). The fluorescence emission spectrum of 12 μM $\alpha_2\beta_2$ serves as a control (c). (B) Titration curves showing the dependence of ANS fluorescence on ANS concentration for (a) E(Ain), (b) E(Ain) + L-Trp, (c) E(Ain) + L-Ser, and (d) E(Ain) + L-Ser + indoline. The predominating enzyme species in these titrations are as follows (see Scheme 1): (a) E(Ain), (b) $E(Aex_2)$ with a trace of $E(Q_3)$, (c) E(A-A) with a trace of $E(Aex_1)$, and (d) the indoline E(Q). The titrations in (a) and (b) were fit to the expression consisting of the sum of two hyperbolic phases. The titrations in (c) and (d) were fit to the expression for a single hyperbolic phase. Conditions and apparent dissociation constants: in each titration, $[\alpha_2\beta_2] = 3.6$ μM; [ANS] was varied from 0 to 0.90 mM. The ligands added and estimated apparent dissociation constants are as follows: (a) none; $K_{d1}' = (62 \pm 15)$ μM and $K_{d2}' > 1$ mM. (b) [L-Trp] = 5 mM, $K_{d1}' = (170 \pm 38)$ μM and $K_{d2}' > 1$ mM. (c) [L-Ser] = 20 mM, $K_d' > 1$ mM. (d) [L-Ser] = 2 mM and [indoline] = 3.5 mM, $K_d' > 1$ mM.

where F_t represents the fluorescence at time t, F_∞ is the final fluorescence, F_i is the fluorescence change of the ith relaxation, and $1/\tau_i$ corresponds to the observed rate for the ith relaxation.

The RSSF measurements have been described previously (Houben et al., 1989; Drewe & Dunn, 1985; Koerber et al., 1983; Brzović & Dunn, 1993, 1995). In each RSSF experiment, a set of 25 scans is collected with delays between scans under programmatic control. The repetitive scan rate is 8.54 ms. In our study, the collection of initial and final scans relative to flow cessation is 8.5 ms and 119.6 s.

RESULTS

ANS Binding. The fluorescence emission of ANS is known to be strongly increased when it is bound to the hydrophobic region of a protein (Stryer, 1965). Upon binding to $\alpha_2\beta_2$ tryptophan synthase, ANS shows significantly enhanced fluorescence, and the emission maximum is shifted from 520 to 480 nm (Figure 1A), indicating either that the ANS molecule is buried in a hydrophobic environment or that it is rigidly confined (Turner & Brand, 1968;

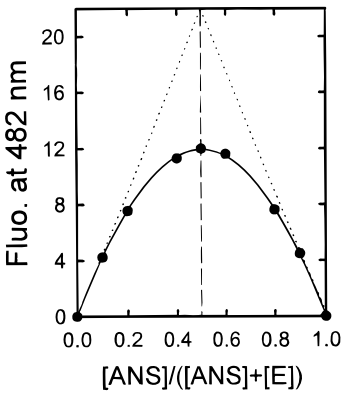

FIGURE 2: Determination of the stoichiometry of ANS binding to E(Ain) according to Job's method of continuous variations at pH 7.8 and 25 °C. The fluorescence intensity of the E(Ain)−ANS complex is plotted vs $\chi = [ANS]_0/\{[ANS]_0 + [\alpha\beta]_0\}$. The vertical dashed line at the abscissa intercept of 0.50 designates a theoretical stoichiometry of 1.0:1.0. The abscissa value of the intersection of the dotted lines (drawn as tangents to the solid line curve at χ values of 0 and 1.0) provides an estimate of the stoichiometry of ANS binding to the high-affinity site of E(Ain). The location of this intersection point is consistent with a stoichiometry of 1 ANS site/$\alpha\beta$ dimeric unit. Conditions: The sum $[\alpha_2\beta_2]_0 + [ANS]_0$ was maintained equal to 50 μM; $\lambda_{ex} = 380$ nm, $\lambda_{em} = 482$ nm.

Slavik, 1982). When a fixed concentration of either E(Ain) or the species produced in the reaction of L-Trp with $\alpha_2\beta_2$ is titrated with ANS, the enhanced fluorescence emission intensity as a function of ANS concentration gives biphasic curves (Figures 1B, curves a and b). For each of these systems, the concentration range between 0 and 0.3 mM ANS is dominated by a moderately high-affinity, hyperbolic phase. At higher ANS concentrations, the curves give evidence of additioanl weak binding interactions likely consisting of multiple sites with $K_d' > 1.0$ mM which may correspond to nonspecific binding interactions. When titrations are carried out for the species formed in the reactions of $\alpha_2\beta_2$ with L-Ser (Figure 1B, curve c) or the quasi-stable qunionoidal species derived from the reaction of indoline with E(A-A) (curve d) (Roy et al., 1988a; see also Figure 6), the resulting curves indicate a very weak affinity for ANS and can be fit by the expression for a single hyperbola. The values of the apparent dissociation constants obtained from these fits are >1.0 mM and appear similar to the low-affinity binding interactions detected for E(Ain) and for the L-Trp system.

Because binding of ANS to E(Ain) consists of a moderately high-affinity interaction together with a much weaker set of interactions (Figure 1B), the method of continuous variations (Job's method) (Job, 1928; Jones & Innes, 1958) was used to investigate the stoichiometry (n) of ANS binding to E(Ain) (Figure 2). Use of this method allows estimates of stoichiometry to be made under conditions where the dominant binding process involves the higher affinity interaction, conditions similar to those used in the experiments which follow. In Figure 2, a representative data set is presented showing the dependence of the fluorescence of the E(Ain)−ANS complex as a function of χ, where $\chi = [ANS]_0/\{[ANS]_0 + [\alpha\beta]_0\}$, and the subscript 0 refers to total concentration. The solid line is the best fit of the experimental points. The dotted lines are drawn as tangents to the solid line at the limiting values of χ (0 and 1.0). The vertical dashed line indicates the abscissa intercept corresponding to a theoretical stoichiometry of 1.0:1.0 (i.e., 1 site/$\alpha\beta$ dimeric unit). The abscissa value of the point of intersection of the tangents indicates that the binding stoichiometry is 1/$\alpha\beta$ dimeric unit within experimental error.

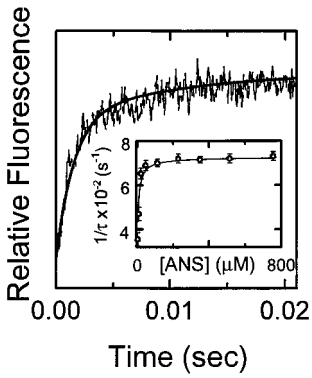

FIGURE 3: Stopped-flow time course for the binding of 50 μM ANS to 12 μM $\alpha_2\beta_2$ measured by ANS fluorescence. The inset shows the dependence of the rate of relaxation ($1/\tau$) on the concentration of ANS.

To assess the potential utility of ANS as a kinetic probe of enzyme−ligand interactions, we investigated ANS binding under rapid-mixing, stopped-flow conditions at pH 7.8 by measuring the ANS fluorescent changes using excitation wavelengths of 380 or 340 nm and an emission window of 450−550 nm. The binding of ANS to the bienzyme complex is a fast process (Figure 3) that is monophasic below 100 μM ANS (kinetic conditions used in the ligand binding studies described in subsequent sections). At much higher ANS concentrations (>100 μM) a second, slower phase appears. The data given in the inset to Figure 3 show that the fast relaxation ($1/\tau_1$) increases as a function of the concentration of ANS and follows a hyperbolic isotherm, increasing from ~350 s^{-1} to a saturated value of 750 s^{-1} with an ANS concentration at half-saturation = 12 μM. This hyperbolic dependence is consistent with a binding mechanism wherein ANS binding is a two-step process involving formation of an initial E(ANS) complex on a time scale too fast to measure, followed by an isomerization to give the fluorescent complex, E*(ANS):

$$E + ANS \underset{k_{-1}}{\overset{k_1}{\rightleftharpoons}} E(ANS) \underset{k_{-2}}{\overset{k_2}{\rightleftharpoons}} E^*(ANS) \qquad K_1 = k_{-1}/k_1 \quad (4)$$

If the binding step is rapid compared to the isomerization step, and provided $[ANS] \gg [\alpha_2\beta_2]$, then

$$1/\tau = \frac{k_2[ANS]}{K_1 + [ANS]} + k_{-2} \quad (5)$$

This kinetic behavior implies that the rapid binding of ANS is followed by a conformational change of the enzyme. Similar effects of bis-ANS on protein conformation have been observed for other proteins (Teschke & King, 1993; Shi et al., 1994). According to eq 5, the initial slope of the plot is $k_2(1/K_1) = (1 \pm 0.2) \times 10^7$ M^{-1} s^{-1}, the y-intercept extrapolated to zero [ANS] is $k_{-2} = (350 \pm 35)$ s^{-1}, and the limiting rate at high [ANS] is $(k_2 + k_{-2}) = (750 \pm 80)$ s^{-1} (Bernasconi, 1976). These quantities yield the following rate and equilibrium values: $k_2 = (400 \pm 40)$ s^{-1}, $k_{-2} = (350 \pm 35)$ s^{-1}, and $K_1 = (4 \pm 0.5) \times 10^{-5}$ M.

Displacement of Enzyme-Bound ANS by L-*Ser,* L-*Ser Analogues, GP, and IGP*. Figure 4A shows the change in the absorption spectrum of the PLP chromophore for the reaction of the $\alpha_2\beta_2$ complex with L-Ser and with L-Trp measured in the presence and in the absence of GP at pH 7.0, all in the presence of 100 mM NaCl. The reaction of

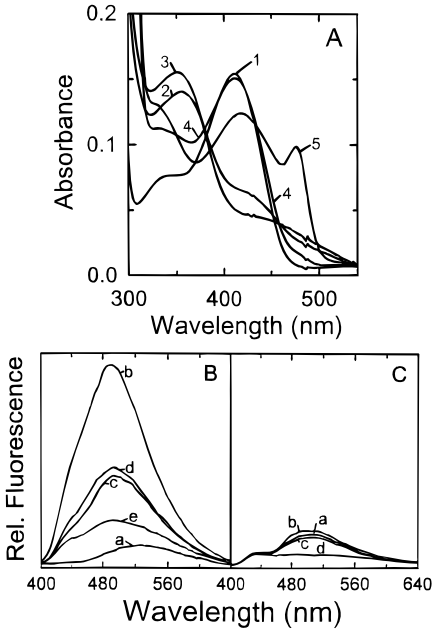

FIGURE 4: Influence of L-Ser, L-Trp, and GP on the absorption spectrum of $\alpha_2\beta_2$ (A) and on the fluorescence of the $\alpha_2\beta_2$−ANS complex (B, C) at pH 7.0. (A) UV−visible spectra of 13 μM $\alpha_2\beta_2$ (1); 13 μM $\alpha_2\beta_2$ and 20 mM L-Ser (2); 13 μM $\alpha_2\beta_2$, 20 mM L-Ser, and 20 mM GP (3); 13 μM $\alpha_2\beta_2$ and 5.3 mM L-Trp (4); and 13 μM $\alpha_2\beta_2$, 5.3 mM L-Trp, and 20 mM GP (5). (B) Fluorescence emission spectra of 13 μM ANS (a) with 10 μM $\alpha_2\beta_2$ either alone (b) or in the presence of 20 mM L-Ser (c) or 20 mM GP (d) or both 20 mM L-Ser and 20 mM GP (e). (C) Control experiments under the same conditions as (B) showing the fluorescence emission spectra of $\alpha_2\beta_2$ alone (a); $\alpha_2\beta_2$ and L-Ser (b); $\alpha_2\beta_2$ and GP (c); and $\alpha_2\beta_2$, L-Ser, and GP (d).

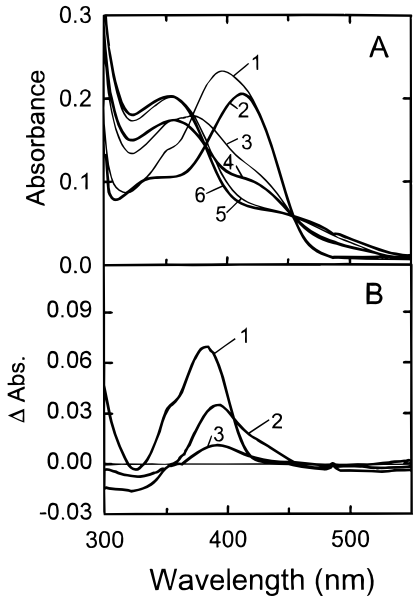

FIGURE 5: Absorption spectra and difference spectra for ANS binding to E(Ain) and to the species formed in the L-Ser reaction with and without GP. (A) The spectrum of 17 μM $\alpha_2\beta_2$ (2) is compared with the spectra obtained upon reaction with 2 mM L-Ser (4) and 2 mM L-Ser + 20 mM GP (6). In (1), (3), and (5), the traces shown are difference spectra obtained by subtracting the spectrum of 157.7 μM ANS in buffer from a mixture of 157.7 mM ANS, 17 μM $\alpha_2\beta_2$ and the following ligands: (1) none; (3) 2 mM L-Ser; (5) 2 mM L-Ser + 20 mM GP. Spectra 1, 3, and 5 show evidence of an additional spectral band at approximately 380 nm due to complex formation between ANS and the enzyme species present. (B) Difference spectra for the binding of ANS calculated by subtraction of the enzyme spectra presented in panel A from the corresponding ANS−enzyme spectra in panel A. Spectrum 1 = A(1) − A(2); spectrum 2 = A(3) − A(4); and spectrum 3 = A(5) − A(6).

L-Ser with enzyme-bound PLP (Figure 4A, spectrum 2) forms an equilibrating mixture consisting of the α-aminoacylate Schiff base complex, E(A-A), with λ_{max} = 350 nm (Scheme 1) and a trace of the external aldimine, E(Aex_1), with λ_{max} = 422 nm. Binding of L-Trp to the enzyme at pH 7.0 (Figure 4A, spectrum 4) gives a distribution of intermediates dominated by the external aldimine, E(Aex_2), with λ_{max} = 425 nm, and a minor amount of the quinonoid, E(Q_3), absorbing at 476 nm. In the L-Ser reaction, the binding of the substrate analogue, GP, to the α subunit shifts the distribution of intermediates from E(Aex_1) to E(A-A) (Figure 4A, spectrum 3). In the L-Trp reaction, GP binding shifts the distribution of E(Q_3) and E(Aex_2) such that the amount of E(Q_3) is slightly increased (Figure 4A, spectrum 5) (Dunn et al., 1990; Brzović et al., 1992b, 1993).

The binding of GP or IGP to the α site and the reactions of substrates and substrate analogues with the β site decreases the characteristic fluorescence of $\alpha_2\beta_2$−ANS, indicating that either the fluorescence is quenched or the dye is displaced (Figure 4B,C). In these and subsequent kinetic experiments to investigate the properties of enzyme-bound ANS complexes, the concentrations of $\alpha_2\beta_2$ and ANS are such that binding is dominated by the high-affinity site. In the kinetic studies, the use of low ANS concentrations (10−15 μM) ensures that only a small fraction of the enzyme molecules contain bound ANS, and therefore ANS qualifies as an indicator or probe of the system (Bernasconi, 1976). Under these conditions, certain combinations of ligands decrease the fluorescence of ANS nearly to the level of free ANS. The changes in the fluorescence of ANS resulting from ligand binding to the α site, or to substrate (or analogue) reaction at the β site (Figures 1, 3, and 4) could be due either to quenching or to a decreased affinity of the resulting enzyme species for ANS. Quenching could arise as a consequence of an altered microenvironment of the ANS binding site or via resonance energy transfer to the PLP chromophore. Comparison of spectra in Figure 4A with those in Figure 4B,C shows that there is significant overlap of the ANS emission spectrum and the absorption spectra of the various PLP-bound enzyme species. Alternatively, if ligand binding to the α site and the interconversion of E(Ain) with the species formed in the reactions of β-site substrates and analogues drives conformational transitions in the protein to states with lowered affinities for ANS, then the decreased fluorescence would be due to dissociation of ANS. Therefore, experiments were undertaken to determine the origins of the decreased fluorescence.

Absorbance measurements of ANS binding to directly detect the formation of ANS−enzyme complexes were undertaken (Figures 5 and 6). The data presented in Figures 1B, 4B, 5, and 6 show that the affinity of the enzyme for ANS is strongly dependent upon the state of ligation of the α site and the covalent form of PLP bound to the β site. When L-Trp reacts at the β site, the resulting spectral changes (Figure 4A, spectrum 4) show that this reaction yields an equilibrating mixture dominated by E(Aex_2). Titration with ANS (Figure 1B, curve b) shows a moderately high affinity interaction (K_d' = 170 ± 38 μM) and multiple weak binding interactions. The ANS fluorescence binding curves for the E(A-A) species formed in the reaction of L-Ser (Figure 1B, trace c) and for the E(Q) species formed from indoline (Figure 1B, trace d) give no evidence of a high-affinity

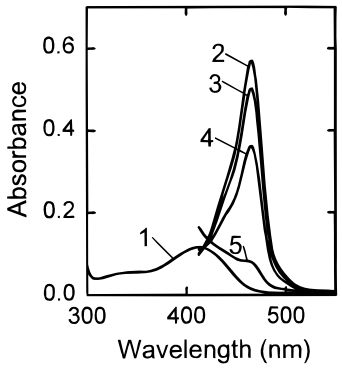

FIGURE 6: Absorption spectra showing the effects of ANS binding on the indoline quinonoid at pH 7.0. Spectra were obtained for the following solutions: (1) 8.2 μM $\alpha_2\beta_2$. (2) 8.2 μM $\alpha_2\beta_2$ + 4 mM L-Ser + 7 mM indoline. Traces 3−5 are difference spectra calculated by subtraction of the spectrum of free ANS from the spectra of the sample shown in spectrum (2) containing 0.124 mM (3), 0.432 mM (4), or 1.40 mM ANS (5), respectively. These difference spectra show that binding of ANS causes a progressive decrease in the quinonoid spectral bands at 468 and 440 nm resulting from redistribution of the PLP-bound intermediates in favor of species absorbing below 430 nm. Due to the high absorbance background below 410 nm from free ANS in spectra 3−5, the region below 410 nm could not be determined.

binding interaction. However, since efficient energy transfer between bound ANS and the PLP chromophores of E(A-A) or E(Q) could result in complete quenching of the ANS fluorescence at a specific, high-affinity site, absorbance studies were undertaken to further investigate ANS binding. ANS binding to hydrophobic and/or molten globule-like protein structures is almost invariably accompanied by a red-shifted absorbance spectrum and a blue-shifted fluorescence emission spectrum with enhanced quantum yield (viz. Figures 1 and 4) (Slavik, 1982). Figure 5 presents absorption spectra and difference spectra for the binding of ANS to E(Ain) (spectra A1 and A2; spectrum B1) and to the species formed in the reaction of L-Ser with E(Ain) both in the absence (spectra A3 and A4; spectrum B2) and presence (spectra A5 and A6; spectrum B3) of GP. Spectra for the quinonoid formed from the reaction of indoline with E(A-A) are given in Figure 6. In the L-Ser system (Figure 5), the reaction proceeds to give E(A-A) as a quasi-stable intermediate in equilibrium with E(Aex_1), and this distribution is pH-dependent, with E(A-A) the favored species at low pH (pH 6−8) (Mozzarelli et al., 1991; Peracchi et al., 1996). The binding of GP to the α site shifts this distribution strongly in favor of E(A-A). The spectra and difference spectra for the ANS-E(Ain) system (Figure 5) show that ANS binding is accompanied by a red shift of the ANS spectrum. In comparison, as indicated by the smaller amplitude of the difference spectrum, the L-Ser system gives species which appear to bind ANS less tightly. The shape of the difference spectrum in the 400−430-nm region is consistent with a weak ANS binding interaction ($K_d' > 1$ mM) which disfavors E(A-A) and stabilizes the E(Aex_1) species ($\lambda_{max} = 425$ nm; Drewe & Dunn, 1985). The absorption spectra for the indoline quinonoid system ($\lambda_{max} = 468$ nm, Figure 6) show that a weak ANS binding interaction ($K_d' > 1$ mM) also disfavors E(Q) and shifts the distribution of intermediates in favor of species absorbing in the 400−430-nm region. The data in Figures 1, 5, and 6 give no evidence of ANS binding to a high, or moderately high, affinity site when the enzyme is in the form of E(A-A) or E(Q).

Table 1: Effect of Ligands on Displacement of ANS in the Absence and Presence of GP[a]

ligands	concn (mM)	apparent ligand dissociation constants at pH 7.8,[b] appK_d^{ligand} (mM) −GP	+GP	% bound ANS displaced[c] pH 7.8 −GP	pH 7.8 +GP	pH 7.0 −GP	pH 7.0 +GP
L-Ser	20	0.0102[d]	<0.01	81	94	88	95
L-Trp	6	0.33[e]	0.026[e]	64	91	35	91
L-His	180	22[f]	4.8[f]	50	73	42	72
Gly	350	25.1[g]	0.92[g]	53	74	39	75
O-Me-Ser[h]	20			54	90	48	90
L-Ser, indoline[h]	2, 3.5			80	92	85	94
		0.131[i]			69		70

[a] Concentrations of $\alpha_2\beta_2$, ANS, and GP are 4 μM, 50 μM, and 20 mM, respectively. [b] These constants correspond to the product of the equilibrium constant for ligand binding and the equilibrium constants for the covalent steps and conformational transformations which comprise the overall equilibrium process measured. [c] Standard error is ±5%. [d] Value taken from Lane and Kirschner (1983). [e] Value taken from Brzović et al. (1992b). [f] Value estimated from Houben and Dunn (1990). [g] Value taken from Brzović et al. (1993). [h] Experiments measured under conditions where the change in ANS fluorescence is independent of the ligand concentration. [i] Values estimated from Figure 7.

The data in Table 1 quantitate the effects of ligand binding and reaction at the α and β sites (Figure 4) on the binding of ANS to the bienzyme complex. The pH 7.0 and 7.8 data in Table 1 give estimates of the percentage of bound ANS displaced when the $\alpha_2\beta_2$−ANS complex is reacted with the ligands and substrates shown. To assure site saturation, conditions were selected such that the ligand concentration used in each instance is at least 5-fold greater than the apparent dissociation constant of the ligand−enzyme complex. Since the fluorescence emission spectrum of bound ANS overlaps with the fluorescence emission spectra of the various enzyme species present (internal aldimine, α-aminoacrylate Schiff base, external aldimines) and with free ANS (viz. Figure 4C), the amount of residual fluorescence due to bound ANS was estimated by correcting for the contributions of the component species. The fluorescence emission spectra used to make these corrections are shown in Figure 4C; this figure shows the emission spectrum of $\alpha_2\beta_2$, together with spectra for the species derived from the reactions of $\alpha_2\beta_2$ with L-Ser, GP, or both L-Ser and GP. For example, to obtain the corrected spectra shown in Figure 4B for the L-Ser reaction, the fluorescence due to bound ANS in the absence of L-Ser was estimated by subtraction of the contributions from the internal aldimine and free ANS (Figure 4C). The amount remaining after reaction with L-Ser was estimated by subtraction of the contributions due to free ANS and to the enzyme-bound L-Ser species measured in separate experiments (Figure 4C).

When either L-Ser, GP, or IGP reacts with the ANS-bound enzyme, the fluorescence of ANS is remarkably decreased, especially at pH 7.0, where the amount of E(Aex_1) present at equilibrium is relatively small (Figure 4B) (Peracchi et al., 1996). The resulting spectra show that L-Ser reaction causes 88% displacement of ANS (spectrum c), while GP binding causes 70% displacement (spectrum d) at pH 7.0 (Table 1). Addition of L-Ser and GP together leads to 95% displacement of the initially bound ANS (Figure 4B, spectrum e). At pH 7.8, the reaction of L-Ser results in the displacement of 81% of the ANS initially bound to $\alpha_2\beta_2$. Results of further tests with L-Trp, L-His, Gly, and O-Me-Ser with and without GP at pH 7.0 and 7.8 are listed in Table

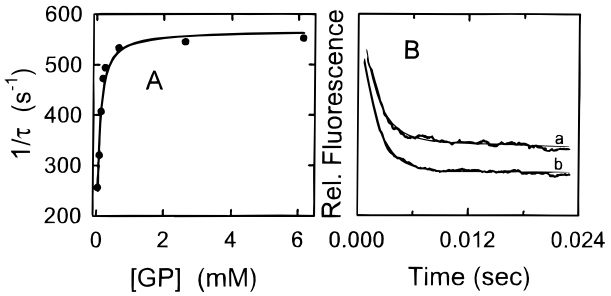

FIGURE 7: Effects of GP and IGP on the displacement of ANS at pH 7.8. (A) Dependence of the relaxation rate ($1/\tau$) for reaction of the ANS−enzyme complex with GP on GP concentration. The reaction mixture consists of 12 μM $\alpha_2\beta_2$, 10 μM ANS, and GP as indicated. (B) Typical time courses for the displacement of ANS by (a) GP or (b) IGP, measured under the condition of 12 μM $\alpha_2\beta_2$, 10 μM ANS, and 5 mM GP or 1 mM IGP.

1. The fluorescence data also show that the reactions of either L-Trp or O-Me-Ser greatly affect the amount of ANS bound in the presence of GP. The amounts of ANS remaining bound are about 10% of the amount initially bound under the conditions used (Table 1). However, reaction of either L-His or Gly has less effect on ANS fluorescence, and the final amount of bound ANS in each instance is approximately 27% of the initial amount.

The dependence of the effects of GP concentration on the time course for ANS displacement at pH 7.8 are shown in Figure 7A. With increasing GP concentration, the relaxation rate ($1/\tau$) increases from ~150 to 560 s^{-1} and follows a hyperbolic isotherm. Typical fluorescence stopped-flow time courses (with excitation wavelength of 380 nm and an emission window of 450−550 nm) for the reactions of GP and IGP are compared in Figure 7B. Comparison of the relative amplitudes and relaxation rates of these time courses show that IGP is slightly more effective than GP in displacing ANS, while the apparent rates are similar. A mechanism involving competition between GP and ANS for the same site can be ruled out. Since ANS displacement occurs in a single-exponential kinetic phase, competition between ANS and GP for the same site would result in a dependence of $1/\tau$ on [GP] that is linear. The hyperbolic form of the curve in Figure 7A contradicts this prediction.

The hyperbolic dependence of the isotherm in Figure 7A is consistent with a GP binding mechanism which involves a binding step followed by a conformational change of the GP−enzyme−ANS complex:

$$E^*(ANS) + GP \overset{K_1^{GP}}{\rightleftharpoons} (GP)E^*(ANS) \underset{k_{-2}^{GP}}{\overset{k_2^{GP}}{\rightleftharpoons}} (GP)E^{**} + ANS \quad (6)$$

where E** represents an enzyme conformation with low affinity for ANS. Since ANS is used as an indicator in this experiment, and, therefore, causes negligible perturbation of GP binding, by analogy to eq 5, the *y*-intercepts at [GP] = 0 and at high [GP], and the initial slope yield values for $k_2^{GP} = (370 \pm 37)$ s^{-1}, $k_{-2}^{GP} = (200 \pm 20)$ s^{-1} and $K_1^{GP} = (1.8 \pm 0.2) \times 10^{-4}$ M.

Reaction of the $\alpha_2\beta_2$ complex with L-Ser was measured both by the change of the ANS fluorescence signal and by the decay of $E(Aex_1)$ fluorescence (Table 2) (Lane & Kirschner, 1983a,b; Drewe & Dunn, 1985). Under the conditions used in Table 2, the formation of $E(Aex_1)$ is a rapid process ($1/\tau_1 = 219 \pm 30$ s^{-1}) (reaction I in Table 2).

Table 2: Relaxation Rate Constants for Formation and Decay of $E(Aex_1)$ and for Displacement of ANS[a]

reaction	signal followed	relaxation Rate (s^{-1})		
		$1/\tau_1$	$1/\tau_2$	$1/\tau_3$
(I) E + L-Ser	$E(Aex_1)$	219 ± 30	13.6 ± 2	2.9 ± 0.5
(II) E(ANS) + L-Ser	ANS		13.6 ± 2	2.9 ± 0.5
(III) ANS displacement[b]	(II)−(I)	220 ± 30	14.0 ± 2	3.0 ± 0.5

[a] The reactions were performed with 12 μM $\alpha_2\beta_2$, 20 mM L-Ser, and (when present) 13 μM ANS at pH 7.0, and an excitation wavelength of 340 nm. [b] The time course for the net displacement of ANS (reaction III) was obtained by subtracting the fluorescence signal in reaction I from the fluorescence signal in reaction II.

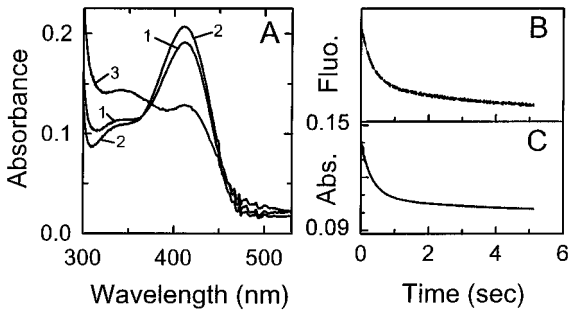

FIGURE 8: Reaction of O-Me-Ser with the $\alpha_2\beta_2$ complex at pH 7.8. (A) RSSF spectra showing the spectrum of 10 μM $\alpha_2\beta_2$ (1) followed by addition of 20 mM O-Me-Ser at 8.5 ms (2) and 119.6 s (3) after mixing. (B) Time course for the reaction of O-Me-Ser with the ANS−$\alpha_2\beta_2$ complex measured by ANS (10 μM) fluorescence. (C) Absorbance time course for the reaction of O-Me-Ser with $\alpha_2\beta_2$ measured by the conversion of the O-Me-Ser $E(Aex_1)$ to E(A-A) at 420 nm.

At pH 7.0, the decay of the $E(Aex_1)$ species to form the E(A-A) complex [monitored by $E(Aex_1)$ fluorescence; λ^{em}_{max} = 490 nm] occurs in a biphasic process (reaction I in Table 2) with $1/\tau_2 = 13.6 \pm 2$ s^{-1} and $1/\tau_3 = 2.9 \pm 0.5$ s^{-1}. When the ANS−enzyme complex is reacted with L-Ser, the reaction time course (reaction II in Table 2) is a composite of the fluorescence changes due to $E(Aex_1)$ conversion to E(A-A) and to the displacement of ANS. The amplitude of the component due to ANS depends on the amount of ANS initially bound. The composite time course (reaction II in Table 2) appears biphasic with $1/\tau_2 = 13.6 \pm 2$ s^{-1} and $1/\tau_3 = 2.9 \pm 0.5$ s^{-1}. Subtraction of the time course measured in the absence of ANS from the time course measured in the presence of ANS yields the time course due to ANS displacement (reaction III in Table 2), a triphasic time course with rates that, within the limits of experimental error, are identical to those observed for the formation and decay of $E(Aex_1)$. When reaction is carried out at pH 7.8, similar results are obtained, but because the increased pH shifts the final distribution of species toward $E(Aex_1)$, the contribution of the fluorescence of this species to the composite signal is increased. Therefore, at pH 7.8 the fluorescence change due to ANS displacement makes a smaller contribution to the observed signal.

Characterization of the Reaction of O-Me-Ser with the $\alpha_2\beta_2$ Complex. Since the ANS and $E(Aex_1)$ fluorescence changes strongly overlap, the timing of ANS displacement with respect to intermediate formation and decay was further examined using an L-Ser analogue, O-Me-Ser, that gives a nonfluorescent E(Aex) species. At pH 7.8, the RSSF spectral changes that occur during the reaction of O-Me-Ser with the $\alpha_2\beta_2$ complex are shown in Figure 8A. The native enzyme (Figure 8A, spectrum 1) is characterized by an absorbance

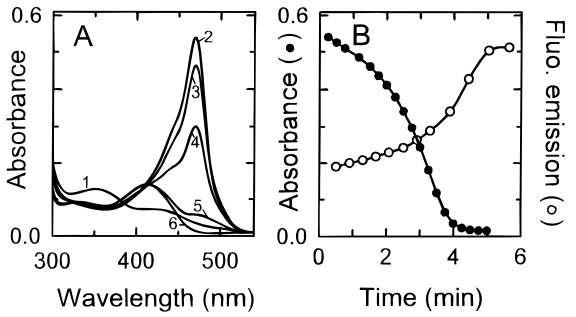

FIGURE 9: Influence of the quinonoid intermediate on ANS fluorescence at pH 7.8. (A) UV−visible spectra of 11 μM $\alpha_2\beta_2$ with 5 mM L-Ser (1) and in the presence of 53 mM β-ME (2−6). Spectra 2−6 were recorded at 0.25, 1.5, 2.5, 3.6, and 5 min after addition of β-ME. (B) Plots of absorbance at 470 nm (●) and fluorescence emission at 482 nm (○) as a function of time. Absorbance data were obtained under the conditions of panel A. Fluorescence data were obtained with 4 μM $\alpha_2\beta_2$, 5 mM L-Ser, and 53 mM β-ME in the presence of 50 μM ANS and using an excitation wavelength of 340 nm.

band at 412 nm with a shoulder at approximately 340 nm. The 412-nm band is derived from the internal aldimine Schiff base formed between the PLP cofactor and the ϵ-amino group of Lys87 at the β active site. Upon mixing with O-Me-Ser, the spectra change rapidly from spectrum 1 to 2, indicating accumulation of an intermediate species. Similar to the L-Ser reaction, the absorbance changes which accompany formation of this species are consistent with formation of the O-methyl analogue of the enzyme-bound external aldimine, E(O-MeAex$_1$). The E(O-MeAex$_1$) species subsequently converts to the quasi-stable aminoacrylate E(A-A) by elimination of methanol (spectrum 3). When measured at 420 nm, the time course for the conversion of E(O-MeAex$_1$) to E(A-A) is biphasic with $1/\tau_1 = (2.8 \pm 0.3)$ s^{-1} and $1/\tau_2 = (0.32 \pm 0.03)$ s^{-1} (Figure 8C).

The reaction of O-Me-Ser with the ANS-enzyme complex also was monitored by ANS fluorescence using an excitation wavelength of 380 nm. The decay of ANS fluorescence is a biphasic process, with $1/\tau_1 = (3.1 \pm 0.3)$ s^{-1} and $1/\tau_2 = (0.32 \pm 0.03)$ s^{-1} (Figure 8B). From comparison of these time courses, it is obvious that the rates and amplitudes of the biphasic processes for decay of E(Aex$_1$) and for the decay of ANS fluorescence are quite similar. Thus, the predominant change in the fluorescence of ANS is concerted with, and coupled to, the conversion of the external aldimine, E(O-MeAex$_1$), to the aminoacrylate E(A-A).

Influence of Quinonoidal Species, E(Q), on ANS Fluorescence. Reaction of β-mercaptoethanol (β-ME) with E(A-A) produces a quinonoid intermediate, which subsequently decays to form the product, *S*-hydroxyethyl-L-cysteine (Goldberg & Baldwin, 1967; Miles, 1979; Drewe et al., 1989). The appearance of the *S*-hydroxyethyl-L-cysteine quinonoid is characterized by an intense absorbance band at 470 nm ($\epsilon \geq 40\,000$ M^{-1} cm^{-1}; Drewe et al., 1989). The spectral changes that accompany the decay of this species reveal that the steady-state level of this quinonoid is gradually converted to products as L-Ser is depleted (Figure 9A). The UV−visible spectral characteristics of the reaction suggest that the final spectrum is composed of an equilibrating mixture of E(Ain) and the *S*-hydroxyethyl-L-cysteine E(Aex) and E(GD) species. Since these species are easily distinguished from E(A-A) and E(Q), we investigated the ANS fluorescence changes in different states of the intermediates upon addition of β-ME to the E(A-A) in the presence of ANS. Under the conditions used, the E(Q) formed from E(A-A) and β-ME rapidly accumulates. However, no enhancement of ANS fluorescence is observed during formation of E(Q). Nevertheless, as this species decays with concomitant accumulation of new species with maximum absorbance at 425 nm, the fluorescence of ANS is enhanced (Figure 9B). This experiment indicates that while the enzyme is in the form of the *S*-hydroxyethyl-L-cysteine quinonoid, either the fluorescence of bound ANS is completely quenched via Forster energy transfer or the quinonoidal species is unable to bind ANS. Since the indoline quinonoid has very low affinity for ANS (Figures 1B and 6 and Table 1), the latter appears to be the correct interpretation. Therefore, ANS binding occurs only as this quinonoid is converted to E(Ain) and the corresponding E(Aex) and E(GD) species.

Scheme 3: Model Depicting the Proposed Ligand-Induced Conformational Changes in the $\alpha_2\beta_2$ Complex That Occur during the Catalytic Cycle of the $\alpha\beta$ Reaction[a]

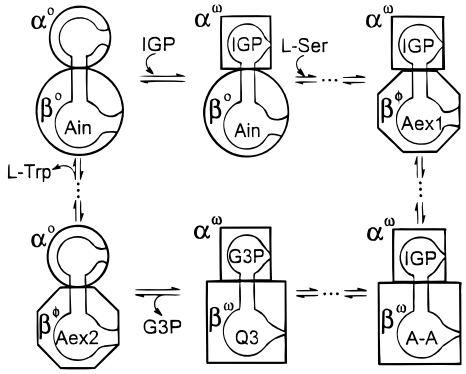

[a] Circles and squares indicate open and closed conformational states, respectively, for both the α and β subunits. Octagons indicate a partially open conformational state of the β subunit (see Table 3).

DISCUSSION

The allosterism exhibited by the tryptophan synthase bienzyme complexes from enteric bacteria functions to achieve the efficient channeling of indole by regulating the conformation states and catalytic states of the α and β catalytic sites of each heterologous dimeric unit of the tetrameric complex (Dunn et al., 1987a,b, 1990; Brzović et al., 1992a,b; Leja et al., 1995; Banik et al., 1995). However, the linkages between the chemical transformations at the α and β sites,[2,3] allosteric signaling, conformational transitions, and substrate channeling have not been clearly established. The allosteric unit is an $\alpha\beta$ dimer. The available evidence indicates the allosteric effects are manifest in the modulation of subunit conformations such that the substrate affinities and catalytic activities of the α and β sites are switched between low-affinity, low-activity states and high-affinity, high-activity states, while the subunits are switched between open and closed conformations (Scheme 3) (Dunn et al., 1990; Brzović et al., 1992b; Leja et al., 1995; Woehl & Dunn, 1995). As depicted in Scheme 3, these events are proposed to occur in a coordinated fashion so that catalysis at the α and β sites is coupled and so that the common

[3] Entry of indole from solution through the α site is inhibited by conversion of the α subunit to a closed conformation in which α-subunit loops 2 and 6 close down over the site in response to the binding of an α-site ligand (GP or G3P) and to E(A-A) formation (Dunn et al., 1990; Brzović et al., 1992a,b, 1993).

metabolite, indole, is prevented from escaping from the confines of the α and β sites and the tunnel. The net result is to ensure the synthesis of L-Trp by efficiently channeling indole from the α site to the β site. The accumulated evidence indicates that the triggers for the switch between alternative conformations of $\alpha\beta$ dimeric units in this allosteric cycle involve two covalent transformations at the β site and ligand binding to the α site (Scheme 3) (Dunn et al., 1990; Lane & Kirschner, 1991; Brzović et al., 1992a,b, 1993; Leja et al., 1995; Banik et al., 1995). Woehl and Dunn (1995) have shown that the binding of a monovalent cation plays an essential role in transmission of these ligand-dependent signals; therefore, this work is restricted to the metal ion-activated form of $\alpha_2\beta_2$. Here, we establish that ANS can be used as a probe of ligand-mediated conformational transitions in the $\alpha_2\beta_2$ oligomer, and we use this probe to correlate the kinetics of the physical and chemical transformations due to ligand binding and reaction with the conformational events triggered by these processes.

Binding of ANS to $\alpha_2\beta_2$ Is Modulated by Ligand Binding and Reaction. The ANS binding isotherm for the E(Ain) species shown in Figure 1B (curve a) is consistent with a single class of noninteracting sites for $\alpha_2\beta_2$ with $K_d' = 62 \pm 15$ μM, together with a class of weak, nonspecific binding interactions. The stoichiometry measured in Figure 2 indicates that the high-affinity binding occurs with a stoichiometry of 1 ANS molecule/$\alpha\beta$ dimeric unit. The evidence for a displacement mechanism involving ligand-driven transitions in the protein to conformational states with lowered affinities for ANS is summarized as follows: (a) The stoichiometry measured for ANS binding gives 1 high-affinity site/$\alpha\beta$ dimeric unit (Figure 2). (b) Ligands specific either for the α site or for the β site, 25 Å away, cause dissociation of ANS from the high-affinity site (Table 1). (c) The hyperbolic dependence of $1/\tau$ for the GP-mediated displacement of ANS implies the binding of GP is followed by a conformational change (Figure 7) and that GP and ANS do not compete for the same site. (d) ANS displacement by β-site amino acid ligands does not correlate with the steric bulk of the side-chain moiety (Table 1).

Consequently, the most likely mechanism for ANS displacement is as follows: prior to ligand binding, the enzyme preexists in two or more conformations, one with moderately high affinity for ANS and one or more with low affinity for ANS. Ligand binding to the α site and substrate reaction at the β site alter the relative stabilities of these conformations in favor of the lower affinity state(s).[2] At subsaturating ANS concentrations, this redistribution brings about a net dissociation of ANS. As documented in Figures 1 and 4−9, ligand binding to the α site and substrate (or analogue) reaction with PLP at the β site either lower the affinity for ANS or abolish binding. This decreased affinity for ANS provides signals that can be used to monitor the kinetics of ligand binding to the α site (Figure 7) and the reactions of substrate at the β site (Figures 8 and 9). While, *a priori*, it might be anticipated that the decreased fluorescence resulting from reaction of the E(Ain)−ANS complex with substrates and substrate analogues is due to resonance energy transfer from bound ANS to the PLP chromophore, the data presented in Figures 1 and 4−6 establish that the affinity of ANS for the E(A-A) and E(Q) species is very weak ($K_{dapp} > 1.0$ mM). Since ANS binding to these enzyme species is negligible at low ANS concentrations, quenching by energy transfer is insignificant. Therefore, the loss of ANS fluorescence upon formation of these intermediates is the consequence of ANS dissociation. The tryptophan synthase β and $\alpha\beta$ reactions are essentially irreversible due to the unfavorable energetics for the conversion of $E(Q_3)$ back to $E(Q_2)$ (Miles, 1991a). Therefore, the reaction of L-Trp with $\alpha_2\beta_2$ gives a stable mixture of intermediates dominated by $E(Aex_2)$. The allosteric effects of GP binding to the α site brings about a redistribution of species with an increased amount of $E(Q_3)$; however, $E(Aex_2)$ is still the dominant species present (Figure 4A) (Houben et al., 1989; Houben & Dunn, 1990; Lane & Kirschner, 1981). As shown in Figure 1B, curve b, ANS binds to this mixture with a $K_{dapp} = (170 \pm 38)$ μM in the absence of GP. The decreased affinity in comparison to E(Ain) results in dissociation of ANS and accounts for the decreased fluorescence signal (Table 1). When GP is added, the fluorescence due to bound ANS is further reduced to a value only slightly higher than that of free ANS, indicating that virtually all of the ANS is displaced.

The dependence of the kinetics of ANS binding to the $\alpha_2\beta_2$ complex on the concentration of ANS (Figure 3) is consistent with the mechanism shown in eqs 4 and 5. When $\alpha_2\beta_2$ is converted to an equilibrating mixture of E(A-A) and $E(Aex_1)$ by reaction with L-Ser (Figures 1 and 4−6 and Table 1), the apparent affinity for ANS is strongly reduced (Figure 1B, curve c); hence at low ANS concentrations, the reaction of L-Ser with $\alpha_2\beta_2$ results in a net displacement of ANS and a decrease in fluorescence. The relatively rapid rates of ANS binding and dissociation (Figure 3) and the sensitivity of ANS fluorescence to ligand binding and reaction at the α and β sites (Figures 4 and 7−9, Tables 1 and 2) render ANS a useful indicator (Bernasconi, 1976) for interrogation of the conformational transition(s) of the $\alpha_2\beta_2$ complex. Although these studies show that the affinity for ANS is dependent on the conformational state of the enzyme, we have been unable to identify the locus of the high-affinity ANS binding site. ANS binds to apolar regions of molten globule proteins and to proteins with hydrophobic binding sites for substrates or cofactors (Handel et al., 1993; Goto & Fink, 1989). Seifert et al. (1984) reported that ANS binds weakly to the isolated β_2 species; this finding suggests that ANS may bind to the β subunit of the $\alpha_2\beta_2$ bienzyme complex. The tunnel between the α and β subunits of tryptophan synthase provides a hydrophobic environment, and, therefore, is one possible site for ANS binding. Ruvinov et al. (1995) have proposed that the much more hydrophobic dye, Nile Red, binds in the tunnel near the β site. Alternatively, ANS may bind to the disordered loop structures that surround the α-subunit catalytic site at or near the $\alpha-\beta$ subunit interface.

ANS Signals Three Distinct Conformational Changes in the $\alpha_2\beta_2$ Complex. Figures 2−9 and Table 1 establish that reactions of certain ligands at either the α or the β sites of tryptophan synthase alter the protein such that the affinity for ANS binding is decreased. In the discussion which follows, and as argued above, these changes in affinity are interpreted to be the consequence of ligand-driven conformation changes and, depending on the ligand type and the extent to which ANS is displaced, fall into three classes. To facilitate this discussion, we use the following nomenclature (see Table 3) to specify the ANS affinity states identified in Figures 2−9 and Tables 1 and 2: E(Ain) with unliganded and liganded α sites is designated as $(\alpha^0\beta^0)_2$ and $(\alpha^\omega\beta^0)_2$, respectively; E(S), E(GD), and E(Aex) species with unliganded and liganded α sites are designated as $(\alpha^0\beta^\phi)_2$ and $(\alpha^\omega\beta^\phi)_2$ respectively; E(A-A) and E(Q) species with un-

Table 3: Summary of ANS Binding Affinities, α-Site Catalytic Activities, and Proposed $\alpha_2\beta_2$ Conformations

proposed $\alpha_2\beta_2$ conformation state	α-site ligation state	β-site covalent state	apparent ANS binding affinity[a] (mM)	relative α-site catalytic activity[b]
$(\alpha^0\beta^0)_2$	unoccupied	(Ain)	0.062[a]	1.00
$(\alpha^0\beta^\phi)_2$	unoccupied	(S), (GD), or (Aex)	0.170[a,c]	1.00
$(\alpha^\omega\beta^\phi)_2$	(GP) or (IGP)[d]	(S), (GD), or (Aex)	>1.0[d]	1.00
$(\alpha^\omega\beta^\omega)_2$	(GP) or (IGP)[d,e]	(A-A)[b] or (Q)[e]	>1.0[d]	27[b] or 4[e]

[a] See Figure 1 and Table 1. Error is estimated as ±24%. [b] Values measured relative to the steady-state rate of cleavage of IGP (α reaction) in the absence of β-site ligands; see Brzović et al. (1992b). [c] Value for the L-Trp external aldimine, E(Aex_2). [d] Although not tested, G3P binding to the α site is expected to exert similar effects on conformation (Brzović et al., 1992b). [e] The rate of 5-nitro-IGP cleavage was used to determine the influence of the indoline quinonoid on α-site catalysis; see Leja et al. (1995).

liganded and liganded α sites are designated as $(\alpha^0\beta^\omega)_2$ and $(\alpha^\omega\beta^\omega)_2$, respectively (Table 3).[2] The rationale for this nomenclature is developed below.

The extent to which the reactions of amino acids cause displacement of ANS by shifting the enzyme to a low-affinity form falls into two classes (Table 1). The amino acid substrates (L-Ser and O-Me-Ser), substrate analogues (Gly, L-His), and the product (L-Trp) all undergo stoichiometric reactions with the β-site PLP cofactor to give equilibrating mixtures of intermediates. The first class involves amino acids which yield either E(A-A) or E(Q) species as the predominant product of reaction (Figures 2, 3, 5, and 6; Tables 1 and 2). These reactions give nearly complete displacement of ANS (>80%) and strongly activate the catalytic activity of the α subunit (Brzović et al., 1992b; Leja et al., 1995; Banik et al., 1995). The second class involves amino acids that give E(S), E(GD), and/or E(Aex) species (i.e., Gly, L-His, or L-Trp). For this class, the amount of ANS displaced is significantly smaller (<64%) (Table 1), and this class does not significantly activate the α subunit (Brzović et al., 1992b). Since the steric bulk of the amino acid side chain varies widely among these amino acids (e.g., from H to $=CH_2$ to indole), there appears to be no direct correlation between ANS displacement and the size of the amino acid side chain (Table 1). *Consequently, displacement of ANS due to ligand binding and reaction at the β site cannot be the result of direct competition between ANS and PLP-bound amino acid for overlapping binding loci, but rather has conformational origins*. These data support designation of the β-subunit conformation state stabilized by E(Ain) as β^0, the conformation stabilized by E(S), E(GD) and E(Aex) species as β^ϕ, and the conformation stabilized by E(A-A) or E(Q) as β^ω (Table 3).

The kinetics studies presented in Table 2 and Figure 8 establish that in the reactions of L-Ser or O-Me-Ser the displacement of ANS is multiphasic. As might be anticipated from the results obtained for Gly, L-His, and L-Trp (Table 1), about 50% displacement occurs as the external aldimines are formed. The remainder is displaced as the external aldimines are converted to E(A-A). The studies of Brzović et al. (1992b) and Woehl and Dunn (1995) established that the conversion of E(Aex_1) to E(A-A) is the process which triggers activation of the α site, and the binding of a monovalent cation is essential to this allosteric transition. *Therefore, we conclude that the displacement of ANS as E(A-A) is formed in the reactions of L-Ser or O-Me-Ser is a consequence of the same conformational transition that is essential for activation of the α site and involves the conversion of β^ϕ to β^ω* (viz. Scheme 3 and Table 3).[2]

The third class of ligand-mediated conformational change involves binding at the α site. As can be seen from Figure 7A, the plot of $1/\tau$ vs [GP] gives a hyperbolic isotherm. This hyperbolic dependence is strong evidence for the existence of a ligand-driven conformational transition and is consistent with a mechanism in which GP initially binds rapidly to give a GP−enzyme−ANS complex which undergoes a slow conformational transition to a second GP−enzyme complex with lowered affinity for ANS (eq 6). If the binding step is faster than the conformation change and if ANS dissociation is concomitant with the conformational transition, then the dependence of the relaxation rate measured by disappearance of ANS fluorescence will be hyperbolic, consistent with Figure 7A (Bernasconi, 1976). IGP binding causes a slightly greater displacement of ANS and gives a similar time course (Figure 7B). *Therefore, we conclude that the displacement of ANS both by α-site and by β-site ligands is a consequence of changes in the conformation of the protein*. These data support the designation of the α-site conformation formed upon binding of GP or IGP as α^ω (Table 3).

Previous studies (Lane & Kirschner, 1981, 1983a,b, 1991; Houben et al., 1989; Houben & Dunn, 1990; Dunn et al., 1987a,b, 1990, Brzović et al., 1992a,b, 1993; Woehl & Dunn, 1995; Peracchi et al., 1996) have shown that the binding of α-site ligands such as G3P, GP, or 3-indolylpropanol 3′-phosphate shifts the distribution of species formed in the L-Ser reaction in favor of E(A-A).[2] Dunn et al. (1990), Brzović et al. (1992a,b, 1993), and Leja et al. (1995) have shown that the combination of GP binding to the α site with E(A-A) formation at the β site drives both sites to closed conformations, here designated as $(\alpha^\omega\beta^\omega)_2$, that inhibit the transfer of indole and indole structural analogues between external solution and the interior of the bienzyme complex (i.e., the α and β sites and the tunnel).[3] The data presented in Figure 4 and Table 1 show that the reaction of amino acids at the β site in combination with GP binding to the α site brings about further displacement of ANS. In the absence of amino acid ligands, GP binding to the α site reduces the amount of bound ANS by 69%. The combinations of GP and L-Ser give 94% displacement, GP and O-Me-Ser give 90%, and GP and L-Trp give 91%, whereas the combinations of GP and Gly, which give 74% displacement, or GP and L-His, which give 73% displacement, show more modest effects. Since in each instance the α sites are saturated with GP and the β-site reactions are stoichiometric, these findings imply that the extent of synergism in ANS displacement exhibited by ligation at the α and β sites depends on the structure of the intermediate at the β site. The α site is not activated by the reactions of Gly, L-His, or L-Trp at the β site; only the formation of E(A-A) or E(Q) activates (Brzović et al., 1992b, Leja et al., 1995; Banik et al., 1995). Therefore, the binding of α-site ligands to the species formed with Gly, L-His, or L-Trp must shift the distribution of conformation states to a closed α site, giving an $(\alpha^\omega\beta^\phi)_2$ species without activating the α site, while the

binding of IGP to E(A-A) transforms the bienzyme complex almost completely to the $(\alpha^{\omega}\beta^{\omega})_2$ conformation, a species with an activated α site. *Therefore, we conclude that both subunits of an αβ subunit pair must be in the closed conformation,* $(\alpha^{\omega}\beta^{\omega})_2$*, to trigger activation (Table 3).*

Open and Closed Conformation Changes Are Triggered by Ligand Binding and Interconversion of Intermediates. According to the hypothesis of Brzović et al. (1992b) (Scheme 3), an open conformation of $\alpha_2\beta_2$ is favored in the absence of ligands. The results presented in Figures 1−9 and Tables 1 and 2 are fully consistent with the conclusion that open conformations bind ANS. As already discussed, certain ligand−protein interactions at either the α or the β sites favor one or another of three conformational states of the bienzyme complex. The reactions of Gly, L-His, or L-Trp give equilibrating mixtures of E(S), E(GD), or E(Aex) species with a conformation state designated as $(\alpha^{0}\beta^{\phi})_2$ (Table 2). Binding of GP or IGP to these species gives an $(\alpha^{\omega}\beta^{\phi})_2$ state with a closed α-site conformation, while binding of GP or IGP to E(A-A) or E(Q) gives a conformation designated as $(\alpha^{\omega}\beta^{\omega})_2$ with both sites closed. These states are distinctly different from each other and from the conformation of the E(Ain) complex. $(\alpha^{0}\beta^{\phi})_2$ and $(\alpha^{\omega}\beta^{\phi})_2$ exhibit α-site catalytic activities that are different from $(\alpha^{\omega}\beta^{\omega})_2$, and each has an affinity for ANS that differs from each other and from E(Ain). $(\alpha^{0}\beta^{\phi})_2$ and $(\alpha^{\omega}\beta^{\phi})_2$ are low-activity forms that retain moderate affinity for ANS; $(\alpha^{\omega}\beta^{\omega})_2$ is a high-activity from that has a low affinity for ANS.

There is considerable evidence that the conformational transitions among $(\alpha^{0}\beta^{\phi})_2$, $(\alpha^{\omega}\beta^{\phi})_2$, and $(\alpha^{\omega}\beta^{\omega})_2$ serve to change (i) substrate binding affinities, (ii) the thermodynamic stability of reaction intermediates, (iii) the access of substrates to the α and β sites and to the tunnel, and (iv) the rates of chemical steps along the catalytic pathway (Kirschner et al., 1991; Miles & McPhie, 1974; Fader & Hammes, 1970, 1971; Houben et al., 1989; Drewe & Dunn, 1985; York, 1972; Dunn et al., 1990; Brzović et al., 1992a,b, 1993; Dunn et al., 1994; Leja et al., 1995; Woehl & Dunn, 1995; Ruvinov et al., 1995; Banik et al., 1995). The ANS fluorescence studies show that conversion of E(Q) to products triggers a change in conformation back to a state that can bind ANS (viz. Scheme 3). *These remarkable findings indicate that the conformation of αβ subunit pairs shift from the closed structure,* $(\alpha^{\omega}\beta^{\omega})_2$*, back to a more open structure,* $(\alpha^{0}\beta^{\phi})_2$*, when E(Q) is converted to the product external aldimine and G3P is released* (Scheme 3). In this context, it is noteworthy that the work of Brzović et al. (1992b) and of Leja et al. (1995) show the conversion of $E(Q_3)$ to $E(Aex_2)$ (Scheme 3) is the allosteric trigger for deactivating the α site. This allosteric switch causes a 30-fold change in the activity of the α reaction. Activation of the α site is linked to the formation of E(A-A), the β-site species which reacts with the channeled intermediate, indole, while deactivation is linked to the conversion of $E(Q_3)$ to $E(Aex_2)$. *Consequently, this switching mechanism provides a means for effectively coupling the activities of the* α *and* β *sites*. This switching has two functions: (i) coupling causes catalysis at the α and β sites to occur in phase, and (ii) the conversion to a closed αβ conformation prevents the escape of indole from the bienzyme complex and ensures its conversion to L-Trp.

Ruvinov et al. (1995) recently have reported that the dye Nile Red binds with enhanced fluorescence at a site proposed to be in the tunnel near the β catalytic site. The circumstantial evidence for this site is based on fluorescence energy transfer between the β-subunit PLP and Nile Red, and the observation that mutation of β-subunit residues near this site alters the fluorescence of Nile Red. The fluorescence of Nile Red also is diminished by the binding of GP to the α site and by reaction of L-Ser at the β site. Ruvinov et al. (1995) speculate that the decrease in Nile Red fluorescence is due to a ligand-induced restriction in the tunnel and that this restriction serves as a gate that regulates the channeling of indole by partially closing the tunnel, thereby converting the β-subunit from an open to a closed form. This is an intriguing suggestion; however, closing the tunnel at a site between the α and β catalytic sites in response to E(A-A) formation would inhibit the transfer of indole and hence would be counterproductive for the channeling of indole between the sites. No such inhibition has been detected. When mixed with indole, the E(A-A) complex reacts very rapidly in a chemically limited step to form $E(Q_3)$ in a process that involves entry of indole through the α site and movement along the tunnel to the β site (Dunn et al., 1987b, 1990; Brzović et al., 1992a,b, 1993; Leja et al., 1995).[3] In our view, the only point in the catalytic cycle where a constriction of the tunnel would facilitate channeling is *after* the L-Trp quinonoid has formed, and this process would need to be reversed in a subsequent step in the cycle preceding the reaction of indole with E(A-A). Since mutations at a variety of loci in the α and β subunits alter the allosteric properties and ligand binding affinities of tryptophan synthase (Brzović et al., 1992a, 1993; Yang & Miles, 1993; Miles, 1991a), the interpretation of the effects of mutations at β-subunit residues on Nile Red fluorescence as evidence for a gating mechanism which controls transfer of indole via the tunnel (Ruvinov et al., 1995) should be viewed with caution.

Mechanism of Substrate Channeling. The accumulated evidence shows the biological function of the tryptophan synthase bienzyme complex is to ensure the synthesis of L-Trp by channeling the common metabolite indole between the two active sites of αβ subunit pairs. The X-ray structure (Hyde et al., 1988) shows that a tunnel connects the two active sites so that the direct transfer of indole can occur. However, in addition to the critically important role played by the tunnel, two additional features are essential to achieve efficient transfer of the common metabolite between the 25 Å distant sites: (a) there must be additional structural constraints to prevent loss of indole to bulk solution, and (b) the catalytic cycles of the two enzymes must occur in phase. As depicted in Scheme 3, these two features of the channeling mechanism are achieved via the dynamic behavior of the bienzyme complex. Through control provided by allosteric signals, αβ subunit pairs are switched between two conformational states, $(\alpha^{0}\beta^{\phi})_2$ and $(\alpha^{\omega}\beta^{\omega})_2$. The low-activity, open conformation, $(\alpha^{0}\beta^{\phi})_2$, allows binding of substrates and release of products. The high-activity, closed conformation, $(\alpha^{\omega}\beta^{\omega})_2$, activates the α site for cleavage of IGP and prevents the escape of indole. The switch from $(\alpha^{0}\beta^{\phi})_2$ to $(\alpha^{\omega}\beta^{\omega})_2$ occurs when $E(Aex_1)$ is converted to E(A-A). Thus, formation of the β-site species, E(A-A), which reacts with the channeled intermediate, indole, is linked to the activation of the α site. The reaction of indole with E(A-A) to form $E(Q_3)$ is ensured by the closed conformation. The switch back to the open conformation is triggered by the conversion of $E(Q_3)$ to $E(Aex_2)$. This transition deactivates the α site and releases G3P. Conversion of $E(Aex_2)$ to L-Trp and E(Ain) at the β site completes the catalytic cycle. Consequently, the subtle

interplay between the architecture and the dynamic properties of this multienzyme complex provide an example of allosteric regulation that functions to achieve substrate channeling.

ACKNOWLEDGMENT

We thank Eilika U. Woehl for helpful discussions and Peter S. Brzović for preliminary experiments with ANS.

REFERENCES

Anderson, K. S., Miles, E. W., & Johnson, K. A. (1991) *J. Biol. Chem. 266*, 8020−8033.
Banik, U., Zhu, D.-M., Chock, P. B., & Miles, E. W. (1995) *Biochemistry 34*, 12704−12711.
Bernasconi, C. (1976) *Relaxation Kinetics*, Academic Press, New York.
Bloxham, D. P. (1973) *Biochemistry 12*, 1602−1608.
Brand, K. (1970) *FEBS Lett. 7*, 235−238.
Brzović, P. S., & Dunn, M. F. (1993), *Bioanalytical Instrumentation 37* (Suelter, C. H., Ed.) pp 191−273, John Wiley and Sons, Inc., New York.
Brzović, P. S., & Dunn, M. F. (1995) *Methods Enzymol. 246*, 168−201.
Brzović, P. S., Miles, E. W., & Dunn, M. F. (1991) in *Proceedings of the 8th International Congress on Vitamin B6 and Carbonyl Catalysis* (Wada, H., Soda, K., Fukui, T., & Kagamiyama, H., Eds.) pp 277−279, Pergamon Press, New York.
Brzović, P. S., Sawa, Y., Hyde, C. C., Miles, E. W., & Dunn, M. F. (1992a) *J. Biol. Chem. 267*, 13028−13038.
Brzović, P. S., Ngo, K., & Dunn, M. F. (1992b) *Biochemistry 31*, 3831−3839.
Brzović, P. S., Hyde, C. C., Miles, E. W., & Dunn, M. F. (1993) *Biochemistry 32*, 10404−10413.
Cheung, H. C. (1969) *Biochim. Biophys. Acta 194*, 478−485.
Daniel, E., & Weber, G. (1966) *Biochemistry 5*, 1893−1900.
Drewe, W. F., Jr., & Dunn, M. F. (1985) *Biochemistry 24*, 3977−3987.
Drewe, W. F., Jr., & Dunn, M. F. (1986) *Biochemistry 25*, 2494−2501.
Drewe, W. F., Jr., Koerber, S. C., & Dunn, M. F. (1989) *Biochimie 71*, 509−519.
Dunn, M. F., Aguilar, V., Drewe, W. F., Jr., Houben, K., Robustell, B., & Roy, M. (1987a) *Ind. J. Biochem. Biophys. 24*, 44−51.
Dunn, M. F., Roy, M., Robustell, B., & Aguilar, V. (1987b) in *Proceedings of the 1987 International Congress on Chemical and Biological Aspects of Vitamin B6 Catalysis* (Korpela, T., & Christen, P., Eds.) pp 171−181, Birkhauser Verlag, Basel, Switzerland.
Dunn, M. F., Aguilar, V., Brzović, P. S., Drewe, W. F., Jr., Houben, K. F., Leja, C. A., & Roy, M. (1990) *Biochemistry 29*, 8598−8607.
Dunn, M. F., Brzović, P. S., Leja, C. A., Pan, P., & Woehl, E. U. (1994) in *Biochemistry of Vitamin B6 and PQQ* (Marino, G., Sannia, G., & Bossa, F., Eds.) pp 119−124, Birkhauser Verlag, Basel, Switzerland.
Faeder, E. F., & Hammes, G. G. (1970) *Biochemistry 9*, 4043−4049.
Faeder, E. F., & Hammes, G. G. (1971) *Biochemistry 10*, 1041−1045.
Goldberg, M. E., & Baldwin, R. L. (1967) *Biochemistry 6*, 2113−2119.
Goto, Y., & Fink, A. L. (1989) *Biochemistry 28*, 945−952.
Handel, T. M., Williams, S. A., & DeGrado, W. F. (1993) *Science 261*, 879−885.
Houben, K. F., & Dunn, M. F. (1990) *Biochemistry 29*, 2421−2429.
Houben, K. F., Kadima, W., Roy, M., & Dunn, M. F. (1989) *Biochemistry 28*, 4140−4147.
Hyde, C. C., Ahmed, S. A., Padlan, E. A., Miles, E. W., & Davies, D. R. (1988) *J. Biol. Chem. 263*, 17857−17871.
Job, P. (1928) *Ann. Chim. 9*, 113−118.
Jones, M. M., & Innes, K. K. (1958) *Anal. Chem. 62*, 1005−1008.
Kawasaki, H., Bauerle, R., Zon, G., Ahmed, S., & Miles, E. W. (1987) *J. Biol. Chem. 262*, 10678−10683.
Kirschner, K., Weischet, W., & Wiskocil, R. L. (1975) in *Protein−Ligand Interactions* (Sund, H., & Blaver, G., Eds.) pp 27−44, Walter de Gruyter, Berlin.
Kirschner, K., Lane, A. N., & Strasser, A. W. M. (1991) *Biochemistry 30*, 472−478.
Koerber, S. C., MacGibbon, A. K. H., Dietrich, H., Zeppezauer, M., & Dunn, M. F. (1983) *Biochemistry 22*, 3424−3431.
Lane, A. N., & Kirschner, K. (1981) *Eur. J. Biochem. 120*, 379−387.
Lane, A. N., & Kirschner, K. (1983a) *Eur. J. Biochem. 129*, 561−570.
Lane, A. N., & Kirschner, K. (1983b) *Eur. J. Biochem. 129*, 571−582.
Lane, A. N., & Kirschner, K. (1991) *Biochemistry 30*, 479−484.
Leja, C. A., Woehl, E. U., & Dunn, M. F. (1995) *Biochemistry 34*, 6552−6561.
Miles, E. W. (1979) *Adv. Enzymol. Relat. Areas Mol. Biol. 49*, 127−186.
Miles, E. W. (1991a) *Adv. Enzymol. Relat. Areas Mol. Biol. 64*, 93−172.
Miles, E. W. (1991b) *J. Biol. Chem. 266*, 10715−10718.
Miles, E. W., & McPhie, P. (1974) *J. Biol. Chem. 249*, 2852−2857.
Miles, E. W., Bauerle, R., & Ahmed, S. A. (1987) *Methods Enzymol. 142*, 398−414.
Miles, E. W., Kawasaki, H., Ahmed, S. A., Morita, H., & Nagata, S. (1989) *J. Biol. Chem. 264*, 6280−6287.
Mozzarelli, A., Peracchi, A., Bettati, S., & Rossi, G. L. (1991) in *Enzymes Dependent on Pyridoxal Phosphate and other Carbonyl Compounds as Cofactors* (Fukui, T., Kagamiyama, H., Soda, K., & Wada, H., Eds.) pp 273−275, Pergamon Press, New York.
Nagata, S., Hyde, C. C., & Miles, E. W. (1989) *J. Biol. Chem. 264*, 6288−6296.
Pauling, L. (1948) *Am. Sci.* 36, 51.
Peracchi, A., Bettati, S., Mozzarelli, A., Rossi, G. L., Miles, E. W., & Dunn, M. F. (1996) *Biochemistry 35*, 1872−1880.
Ploug, M., Ellis, V., & Danø, K. (1994) *Biochemistry 33*, 8991−8997.
Roy, M., Keblawi, S., & Dunn, M. F. (1988a) *Biochemistry 27*, 6698−6704.
Roy, M., Miles, E. W., Phillips, R. S., & Dunn, M. F. (1988b) *Biochemistry 27*, 8661−8669.
Ruvinov, S. B., Yang, X.-J., Parris, K. D., Banik, U., Ahmed, S. A., Miles, E. W., & Sackett, D. L. (1995) *J. Biol. Chem. 270*, 6357−6369.
Slavik, J. (1982) *Biochim. Biophys. Acta 694*, 1−25.
Siefert, T., Bartholmes, P., & Jaenicke, R. (1984) *Z. Naturforsch. C 39*, 1008−1011.
Shi, L., Palleros, D. R., & Fink, A. L. (1994) *Biochemistry 33*, 7536−7546.
Stryer, L. (1965) *J. Mol. Biol. 13*, 482−495.
Turner, D. C., & Brand, L. (1968) *Biochemistry 7*, 3381−3390.
Teschke, C. M., & King, J. (1993) *Biochemistry 32*, 10839−10847.
Woehl, E. U., & Dunn, M. F. (1995) *Biochemistry 34*, 9466−9476.
Yang, X.-J., & Miles, E. W. (1993) *J. Biol. Chem. 268*, 22269−22272.
Yanofsky, C. (1967) *Harvey Lect. 61*, 148−168.
Yanofsky, C., & Crawford, I. P. (1972) in *The Enzymes, 3rd Ed.* (Boyer, P. D., Ed.) pp 1−31, Academic Press, New York.
York, S. S. (1972) *Biochemistry 11*, 2733−2740.
Yutani, K., Ogasashara, K., Tsujita, T., & Sugono, Y. (1987) *Proc. Natl. Acad. Sci. U.S.A. 84*, 4441−4444.

BI960033K